



HAL
open science

LPS-enriched small extracellular vesicles from metabolic syndrome patients trigger endothelial dysfunction by activation of TLR4

Sakina Ali, Marine Mallocci, Zainab Safiedeen, Raffaella Soleti, Luisa Vergori, Xavier Vidal-Gómez, Charlène Besnard, Séverine Dubois, Soazig Le Lay, Jérôme Boursier, et al.

► To cite this version:

Sakina Ali, Marine Mallocci, Zainab Safiedeen, Raffaella Soleti, Luisa Vergori, et al.. LPS-enriched small extracellular vesicles from metabolic syndrome patients trigger endothelial dysfunction by activation of TLR4. *Metabolism*, 2021, 118, pp.154727. 10.1016/j.metabol.2021.154727 . hal-03284090

HAL Id: hal-03284090

<https://univ-angers.hal.science/hal-03284090>

Submitted on 26 Oct 2021

HAL is a multi-disciplinary open access archive for the deposit and dissemination of scientific research documents, whether they are published or not. The documents may come from teaching and research institutions in France or abroad, or from public or private research centers.

L'archive ouverte pluridisciplinaire **HAL**, est destinée au dépôt et à la diffusion de documents scientifiques de niveau recherche, publiés ou non, émanant des établissements d'enseignement et de recherche français ou étrangers, des laboratoires publics ou privés.



LPS-enriched small extracellular vesicles from metabolic syndrome patients trigger endothelial dysfunction by activation of TLR4

Sakina Ali^a, Marine Mallocci^a, Zainab Safiedeen^a, Raffaella Soleti^a, Luisa Vergori^a, Xavier Vidal-Gómez^a, Charlene Besnard^a, Séverine Dubois^{a,b}, Soazig Le Lay^a, Jérôme Boursier^b, Arnaud Chevrollier^{b,c}, Frédéric Gagnadoux^{a,b}, Gilles Simard^{a,b}, Ramaroson Andriantsitohaina^{a,b}, M. Carmen Martinez^{a,b,*},
On behalf of Metabol study Group

^a SOPAM, U1063, INSERM, UNIV Angers, SFR ICAT, Angers, France

^b Centre Hospitalo-Universitaire d'Angers, France

^c Institut MITOVASC, CNRS 6015, INSERM U1083, UNIV Angers, SFR ICAT, Angers, France

ARTICLE INFO

Article history:

Received 9 November 2020

Accepted 8 February 2021

Available online xxxx

Keywords:

Exosomes

Metabolic syndrome

Insulin resistance

Endothelial dysfunction

TLR4/LPS axis

ABSTRACT

Background: Metabolic syndrome (MetS) is characterized by a cluster of interconnected risk factors -hyperglycemia, dyslipidemia, hypertension and obesity- leading to an increased risk of cardiovascular events. Small extracellular vesicles (sEVs) can be considered as new biomarkers of different pathologies, and they are involved in intercellular communication. Here, we hypothesize that sEVs are implicated in MetS-associated endothelial dysfunction.

Methods: Circulating sEVs of non-MetS (nMetS) subjects and MetS patients were isolated from plasma and characterized. Thereafter, sEV effects on endothelial function were analyzed by measuring nitric oxide (NO) and reactive oxygen species (ROS) production, and mitochondrial dynamic proteins on human endothelial aortic cells (HAoECs).

Results: Circulating levels of sEVs positively correlated with anthropometric and biochemical parameters including visceral obesity, glycaemia, insulinemia, and dyslipidemia. Treatment of HAoECs with sEVs from MetS patients decreased NO production through the inhibition of the endothelial NO-synthase activity. Injection of MetS-sEVs into mice impaired endothelium-dependent relaxation induced by acetylcholine. Furthermore, MetS-sEVs increased DHE and MitoSox-associated fluorescence in HAoECs, reflecting enhanced cytosolic and mitochondrial ROS production which was not associated with mitochondrial biogenesis or dynamic changes. MetS patients displayed elevated circulating levels of LPS in plasma, and, at least in part, it was associated to circulating sEVs. Pharmacological inhibition and down-regulation of TLR4, as well as sEV-carried LPS neutralization, results in a substantial decrease of ROS production induced by MetS-sEVs.

Conclusion: These results evidence sEVs from MetS patients as potential new biomarkers for this syndrome, and TLR4 pathway activation by sEVs provides a link between the endothelial dysfunction and metabolic disturbances described in MetS.

© 2021 Elsevier Inc. All rights reserved.

Abbreviations: BMI, body mass index; DHE, dihydroethidium; eNOS, endothelial NO-synthase; EPR, electronic paramagnetic resonance; EV, extracellular vesicle; HAoECs, human aortic endothelial cells; HOMA, homeostatic model assessment; IEVs, large extracellular vesicles; LPS, lipopolysaccharide; MetS, metabolic syndrome; nMetS, non-metabolic syndrome; NO, nitric oxide; NTA, nanoparticle tracking analysis; PA, palmitic acid; PBS, phosphate-buffered saline; ROS, reactive oxygen species; sEVs, small extracellular vesicles; SNP, sodium nitroprussiate; TLR4, toll-like receptor 4; VSMC, vascular smooth muscle cells.

* Corresponding author at: INSERM UMR 1063, Stress Oxydant et Pathologies Métaboliques, Institut de Biologie en Santé, 4 rue Larrey, F-49933 Angers, France.

E-mail address: carmen.martinez@univ-angers.fr (M.C. Martinez).

1. Introduction

Metabolic syndrome (MetS) is a worldwide public health problem, characterized by a cluster of interconnected risk factors including hyperglycemia, dyslipidemia, hypertension and obesity, leading to an increased risk of cardiovascular events. Endothelial dysfunction actively participates in the development of cardiovascular diseases associated with MetS [1]. Among the main actors associated with the endothelium injury, extracellular vesicles (EVs) are involved in the pathogenesis and maintenance of cardiovascular and metabolic diseases [2–4]. EVs, that carry proteins, lipids and nucleic acids, can act as biological vectors through their interaction with their target cells. Two main types of

EVs have been described: microvesicles or large EVs (IEVs) formed by budding of the plasma membrane, and exosomes or small EVs (sEVs) originated from the endosomal compartment [4].

Due to their strategic location, endothelial cells are the first target cells of circulating EVs. Regarding MetS, we have described that circulating IEVs from MetS (MetS-IEVs) patients induce endothelial dysfunction characterized by a decrease of nitric oxide (NO) production associated with the inhibition of endothelial NO-synthase (eNOS), and an increase in oxidative and nitrate stresses [5]. Furthermore, we have shown that MetS-IEVs carry Fas-ligand and interact with Fas in endothelial cells. This induces a temporal crosstalk between endoplasmic reticulum and mitochondria with respect to spatial regulation of reactive oxygen species (ROS) production *via* the neutral sphingomyelinase. All of these events lead to a reduction of NO bioavailability accounting for the subsequent impairment of endothelium-dependent vasorelaxation [6].

Several studies have suggested that sEVs could be also biomarkers for metabolic diseases [7]. Indeed, it has been demonstrated that circulating cystatin c-associated sEVs rate is positively correlated with (i) an increase of inflammation, (ii) a decrease of HDL-cholesterol and (iii) the prevalence of MetS [8]. In addition, miR-197, miR-23a and miR-509-5p content of sEVs of patients with MetS has been reported to correlate with body mass index (BMI) and may be considered as potential contributors of dyslipidemia in MetS [9]. Although the role of sEVs in the development of MetS has been suggested [10], currently, the effects of these vesicle subtypes on the endothelial function have not been studied yet.

Thus, the aim of the present study was firstly to characterize circulating sEVs from nMetS subjects and patients with MetS. Correlations of their levels with anthropometric and biochemical parameters were assessed to analyze their potential relevance as biomarkers. Secondly, we determined *in vitro* effects of sEVs from MetS patients (MetS-sEVs) on endothelial molecular pathways implicated in NO and ROS productions. Finally, sEVs were injected intravenously into mice to test their *in vivo* pathophysiological relevance.

2. Materials and methods

2.1. Patients

This study was approved by the ethics committee of the University Hospital of Angers (France). nMetS subjects and MetS patients were recruited in the NUMEVOX cohort (NCT: 00997165) at the Department of Endocrinology and Nutrition of the University Hospital of Angers. After cohort participants gave their informed consent, they were characterized according to these unified criteria [11]. Patients were identified as MetS when they displayed at least three of the following five criteria: i) waist circumference > 102 or 88 cm for men and women, respectively; ii) systolic and diastolic blood pressure \geq 130/85 mmHg; iii) fasting glycemia \geq 1.0 g/l; iv) triglycerides \geq 1.5 g/l; and v) high-density cholesterol lipoprotein < 0.4 g/l in men or < 0.5 g/l in women. For the present study, patients with preexisting chronic inflammatory disease or cancer were excluded. A total of 102 subjects were identified as MetS patients and 75 subjects who displayed two or less MetS criteria were identified as nMetS subjects. Baseline characteristics and clinical data of nMetS subjects and MetS patients are summarized in Supplemental Table 1.

2.2. sEV isolation

Peripheral blood (20 ml) from nMetS or MetS patients was collected in EDTA tubes (Vacutainers; Becton Dickinson, Le Pont de Claix, France) from a peripheral vein using a 21-gauge needle to minimize platelet activation and was processed within 2 h. After a 20 min centrifugation at 270g, platelet-rich plasma was separated from whole blood. Then, platelet-rich plasma was centrifuged for 20 min at 1500g to obtain platelet-free plasma (PFP). Remaining PFP was centrifuged at 21,000g for 45 min to remove IEVs. The supernatant was centrifuged at

100,000g (Optima MAX-XP ultracentrifuge and MLA-80 rotor, Beckman Coulter, Villepinte, France) for 70 min to pellet sEVs. Then, sEVs were washed in phosphate-buffered saline (PBS) (NaCl 137 mM, KCl 2.7 mM, Na₂HPO₄ 10 mM, KH₂PO₄ 1.8 mM, pH = 7.4) and re-centrifuged at 100,000g for 70 min. Finally, sEVs pellet were resuspended in 200 μ l of PBS and stored at 4 °C until subsequent use.

2.3. Transmission electronic microscopy

sEV preparations were first fixed overnight at 4 °C with 2.5% glutaraldehyde (LFG Distribution, Lyon, France) in 0.1 M PBS. Then, sEVs were washed two times in PBS by 100,000g centrifugation for 70 min. sEVs were resuspended in milliQ water and 20 μ l were deposited on Formvar®-coated copper grids for 2 min. sEVs were negatively stained with 20 μ l of uranyl acetate 5% (diluted in ethanol 50%) for 30 s. Grids were rinsed briefly with milliQ water and left to air dry. Grids were then observed with a Jeol JEM 1400 microscope (Jeol, Croissy sur Seine, France) operated at 120 keV.

2.4. Determination of sEV size and concentration by nanoparticle tracking analysis (NTA)

sEV samples were diluted in sterile NaCl 0.9% prior to NTA (NanoSight NS300, Malvern Instruments Ltd., Malvern, UK) equipped with a 405 nm laser. Five videos of 60 s were recorded per sample with optimized set parameters. Temperature was automatically monitored and ranged from 20 °C to 21 °C. Videos were analyzed when a sufficient number of valid trajectories was measured. Results presented correspond to the mean of the 5 videos taken for each biological sample. sEV concentrations were normalized by the collected plasma volume for each patient. Data capture and further analysis were performed using the NTA software version 3.1.

2.5. Cell culture

Human aortic endothelial cells (HAoECs, Promocell, Heidelberg, Germany) were cultured in endothelial cell growth medium MV2 (Promocell) supplemented with 1% streptomycin/penicillin (Lonza, Basel, Switzerland). Cells were treated for 4 or 24 h with sEVs from nMetS subjects (nMetS-sEVs) or MetS-sEVs at different concentrations (5, 10 or 20 μ g/ μ l). Preliminary studies showed that, at 20 μ g/ml, sEVs-MetS abolished NO production leading to HAoEC death (Supplemental Fig. 1A), whereas at 10 μ g/ml, a reduction of 50% on NO production was observed without cell death. This concentration corresponded to $7 \times 10^5 \pm 2 \times 10^5$ and $1.9 \times 10^6 \pm 4 \times 10^5$ sEVs/ μ l of circulating sEVs for nMetS subjects and MetS patients, respectively. In consequence, the chosen work concentration of sEVs for experiments was 10 μ g/ml. To scavenge mitochondrial ROS, mitoTEMPO (25 nM, Santa Cruz Biotechnology, Dallas, TX) was pre-incubated for 30 min before sEV treatments. In other set of experiments, HAoECs were serum starved for 2 h before treatment with sEVs or palmitic acid (PA, Sigma-Aldrich, St. Quentin, Fallavier, France) at 300 μ M for 24 h: then, cells were stimulated with 100 nM insulin for 5 min. To assessed Toll-like receptor 4 (TLR4) expression, cells were treated for 4 h with nMet-sEVs, MetS-sEVs or lipopolysaccharide from *Escherichia coli* O55:B5 (LPS, Sigma-Aldrich) at 200 ng/ml before protein extraction.

2.6. sEV internalization

Isolated sEVs were stained with PKH67-dye (Sigma Aldrich) in agreement with the manufacturer's procedure. Briefly, sEVs were incubated with 2 mM PKH67-dye in PBS for 2 min at room temperature. An equal volume of fetal bovine serum was added to stop staining. Then, sEVs were centrifuged at 100,000g for 70 min to remove the supernatant. The sEV pellet was resuspended in PBS and HAoECs were incubated with PKH67-labeled sEVs either for 4 or 24 h at 37 °C. At the end of incubation,

cells were fixed with 4% paraformaldehyde for 20 min followed by staining with tetramethylrhodamine isothiocyanate-phalloidin (50 mg/ml, Sigma-Aldrich) for 90 min at room temperature. After washing with PBS, nuclei were stained with DAPI for 5 min and cells were mounted and visualized with confocal microscopy (CLMS700, Zeiss, ZENsoftware). All images were acquired using a x63 objective.

2.7. Nitric oxide (NO) and superoxide anion (O_2^-) determination by electronic paramagnetic resonance (EPR)

The detection of NO production was performed using the technique with Fe^{2+} diethyldithiocarbamate (DETC; Sigma-Aldrich) as spin trap, as previously described [6]. After sEV treatment, cells were incubated with 300 μ l of colloid $Fe(DETC)_2$ (400 μ M) at 37 °C for 45 min. The detection of O_2^- production was performed by EPR technique using 1-hydroxy-3-methylcarbonyl-2, 2, 5, 5 tetramethyl pyrrolidine (CMH) (Noxygen, Mainz, Germany) as spin trap. Cell culture medium was replaced with 500 μ l of deferoxamine-chelated Krebs-Hepes solution containing CMH (500 μ M), deferoxamine (25 μ M, Sigma-Aldrich), and sodium diethylthiocarbamate (5 μ M, Sigma-Aldrich), and incubated for 45 min at 37 °C. After spin trap incubation, cells were then scrapped and frozen in plastic tubes and analyzed in a Dewar flask by EPR spectroscopy. NO and O_2^- measurements were performed on a tabletop x-band spectrometer miniscope (MS200; Magnettech, Berlin, Germany). The quantitative measurement of NO and O_2^- signal amplitudes were reported to protein concentration of each sample. Results are expressed in percentage compared to the control condition.

2.8. Western blotting

Purified sEVs or lEVs (15 μ g), 20 μ g of proteins from lysed cells or from mesenteric arteries from female mice treated with sEVs were separated on 4–12% NuPage gels (ThermoFisher Scientific, Rockford, IL) and transferred on nitrocellulose blotting membrane (Amersham, Little Chalfont, UK). To characterize sEVs, blots were probed with anti-CD63, CD81, CD9 and TSG101 (Santa Cruz Biotechnology, Dallas, TX), ALIX (BioLegend, San Diego, CA), LPS (ThermoFisher Scientific) and GAPDH (Abcam, Cambridge, UK). In other set of experiments, blots were probed with anti-eNOS (BD Biosciences, San Jose, CA), phospho-eNOS Ser 1177, phospho-eNOS Thr 495, AKT and phospho-AKT Ser 473 (Cell Signaling, Beverly, MA, respectively), and LPS and TLR4 (Santa Cruz Biotechnology). Finally, blots were probed with anti-PGC1 α , Mfn1 and Mfn2 (Abcam), Fis1 (Santa Cruz Biotechnology), and OPA1 (BD Biosciences). A polyclonal mouse anti-human β -actin antibody (Sigma-Aldrich) was used for standardization of protein gel loading.

2.9. Animal model

All animal studies were performed according institutional protocols (n°APAFIS#22561). Swiss male and female mice (8 to 10 week-old) were treated *in vivo* by intravenous injection of sEVs at 10 μ g/ml of blood into the tail vein for 24 h, as previously described [5,6]. Aorta and mesenteric arteries were isolated and fat removed for further experiments.

2.10. Vascular reactivity

After 24 h, aorta from male mice were isolated and aortic rings were mounted on a wire myograph. Endothelium-dependent relaxation was studied by cumulative application of acetylcholine (1 nM to 10 μ M, Sigma-Aldrich) in aortas with functional endothelium pre-contracted with U46619 (Sigma-Aldrich). The functionality of aortic smooth muscle cells was assessed by studying vascular relaxation in response to sodium nitroprusside (1 nM to 3 μ M, Sigma-Aldrich). Vascular sensitivity was quantified by means of $pD_2 = -\log EC_{50}$, EC_{50} being the molar concentration of the agonist that produces 50% of the maximal effect; EC_{50} values were calculated by logit-log regression.

2.11. Measurement of oxidative stress by confocal microscopy

HAoECs were grown on glass slides (Ibidi, Martinsried, Germany) and were treated for 4 h with sEVs from MetS or nMetS subjects at 10 μ g/ml, or LPS at 200 ng/ml. To inhibit TLR4, TAK-242 (5 μ M, Sigma-Aldrich) was added to cells for 1 h before treatments with sEVs. To knock-down TLR4 protein expression, HAoECs were transfected with siRNAs against TLR4 (Santa Cruz Biotechnology) for 24 h before sEV treatments. A scrambled siRNA (Santa Cruz Biotechnology) was used as negative control. To block the effect of LPS carried by sEVs, 100 μ M of polymyxin B (Santa Cruz Biotechnology) was added to isolated sEVs for 1 h before their pelleting by using ExoQuick (System Biosciences, Palo Alto, CA) followed by their centrifugation at 1500g for 30 min. Cells were treated with sEVs containing polymyxin B for 4 h before their incubation with either the oxidative fluorescent dye dihydroethidium (DHE, 5 μ M, Sigma-Aldrich) for 30 min at 37 °C or MitoSox red (5 μ M, Molecular Probes, Eugene, OR) for 10 min at 37 °C. Finally, cells were fixed by 4% paraformaldehyde for 20 min at room temperature and DAPI (Sigma-Aldrich) was added for 5 min. All images were acquired using x20 objective with confocal microscopy (CLMS 700, Zeiss, ZEN software).

In other set of experiments, 24 h after intravenous injection of sEVs, aortic rings from female mice were incubated 30 min with DHE or 10 min with MitoSox red before being included in OCT (Sakura Finetek, Terrace, CA). Ten μ m sections of aorta were cut with a cryostat (Leica CM1900, Heidelberg, Germany) and mounted on slide using mounting medium supplemented with DAPI (ThermoFisher Scientific). Aorta sections were visualized with confocal microscopy using x20 objective.

2.12. Quantitative real-time reverse transcription-polymerase chain reaction (RT-PCR) analysis

HAoECs were treated either with vehicle (PBS), sEVs from nMetS or MetS patients (10 μ g/ml) for 24 h, then frozen in liquid N₂. Mitochondrial DNA (mtDNA) copy number was determined by qPCR using ND5 and β -actin genes as respective markers of the copy number of mitochondrial and genomic DNA (primer sequences in Supplementary Table 1). Total DNA was isolated from HAoECs (Macherey Nagel, Düren, Germany) and RT-PCR analyses were performed using a Chromo4™ (Bio-Rad, Marnes la-Coquette, France) and SYBR Green detection (Bio-Rad). Quantifications were realized according to the Ct method. Results were normalized with mRNA expression of β -actin.

2.13. Citrate synthase activity

The reaction capacity of the citrate synthase was followed by measuring the formation of the -SH group released from CoA-SH using of the reactive Ellman reagent (5,5'-dithiobis [2-nitrobenzoic]), DTNB (Sigma-Aldrich). HAoECs were untreated or treated with sEVs from nMetS and MetS patients for 24 h, then frozen in liquid N₂. Cells were resuspended in buffer (sucrose 250 mM, Trizma 20 mM, EDTA 2 mM, pH 7.2) and samples were incubated with DTNB (150 μ M), oxaloacetate (500 μ M, Sigma-Aldrich), acetyl-CoA (300 μ M, Sigma-Aldrich) and 0.1% of Triton X-100 (Sigma-Aldrich), during 2 min at 37 °C. Activity was measured by absorbance at 412 nm and normalized by the amount of protein of each sample.

2.14. Plasma endotoxin assay

Plasma LPS concentrations were measured using a Pierce Chromogenic Endotoxin Quant Kit (ThermoFisher Scientific). LPS assay was performed with PFP of nMetS and MetS patients. Briefly, 50 μ l of plasma was diluted 1:5 to 1:10 with endotoxin-free water, then heat inactivated at 70 °C for 10 min. Fifty μ l of diluted sample was added to 96-well culture plate and remaining procedures were performed according to the supplier's instructions. Endotoxin concentrations (EU/

ml) in the samples were determined from a standard curve using pure endotoxin standards.

2.15. Data analysis

Data normality was assessed using the Kolmogorov-Smirnov test. Statistical analysis was performed either by using Student's *t*-tests for single comparisons or ANOVA followed by Tukey post-hoc test for multiple comparisons. In cases where normality was not confirmed, statistical analysis from two groups and more than two groups were analyzed by Mann-Whitney *U* test, and analysis of variance for repeated measures and subsequent Bonferroni test post-hoc, respectively. Correlations were analyzed by Spearman correlation test. Data are represented as mean \pm SEM, *n* represents the number of donors. ≤ 0.05 was considered statistically significant. Statistical analysis was performed using GraphPad Prism (version 5.0; GraphPad Software Inc., San Diego, CA).

3. Results

3.1. Characterization of subjects of the study

MetS patients were significantly older than nMetS subjects and exhibited a significant increase in BMI, waist and hip circumferences, systolic blood pressure, glycemia, insulinemia, HOMA and triglyceride levels, and decreased plasma HDL levels (Table 1). These data indicate that MetS displayed visceral obesity, hypertension, insulin resistance and dyslipidemia.

3.2. Characterization of circulating sEVs

Isolated sEVs from both nMetS and MetS patients expressed specific exosomal markers such as ESCRT-associated proteins (ALIX, TSG101) and tetraspanins (CD63, CD81 and CD9) (Fig. 1A). sEVs did not express GAPDH, a specific protein found in IEVs (Supplemental Fig. 1B). As illustrated in Fig. 1B, sEVs had a round shape and a size of ~60 nm (Fig. 1B).

3.3. Circulating rate and size of sEVs are correlated with metabolic disorders

Size of sEVs measured as mode and mean was significantly decreased in patients with MetS compared to nMetS subjects (Fig. 1C–E) and this reduction was associated with the increase of number of MetS criteria

Table 1
Baseline characteristics of metabolic syndrome patients (MetS) compared to non-metabolic syndrome subjects (nMetS).

	nMetS	MetS	<i>P</i>
Number	75	102	
Mean age (years)	48.3 \pm 1.5	55.8 \pm 1.1	<0.0002
Sex ratio (male/female)	41/34	57/45	
Body Mass Index (kg/m ²)	25.2 \pm 0.5	33.3 \pm 0.6	<0.0001
Waist circumference (cm)	88.3 \pm 1.6	111.0 \pm 1.4	<0.0001
Hip circumference (cm)	99.1 \pm 1.3	111.7 \pm 1.2	<0.0001
Systolic blood pressure (mm Hg)	122.2 \pm 1.5	128.9 \pm 1.5	0.0007
Diastolic blood pressure (mmHg)	76.6 \pm 1.3	78.4 \pm 1.2	NS
Glycemia (g/L)	0.93 \pm 0.02	1.18 \pm 0.03	<0.0001
Insulinemia (μ U/L)	6.7 \pm 0.5	16.2 \pm 1.3	<0.0001
HOMA	1.51 \pm 0.14	4.8 \pm 0.5	<0.0001
Total cholesterol (g/L)	1.94 \pm 0.08	1.95 \pm 0.07	NS
HDL (g/L)	0.54 \pm 0.02	0.46 \pm 0.01	<0.0001
LDL (g/L)	1.21 \pm 0.05	1.08 \pm 0.04	NS
Triglycerides (g/L)	0.86 \pm 0.03	1.7 \pm 0.1	<0.0001
Treatments (%)			
Oral antidiabetic	6.6	49	
Anti-hypertensive	17	60	
Statin	9	35	

The homeostatic model assessment (HOMA) is a method used to quantify insulin resistance (HOMA = glycemia \times insulinemia / 22.5).

(Fig. 1F). Moreover, sEV size expressed as mode or mean was negatively correlated with the increase of weight, waist circumference, BMI, glycemia and levels of triglycerides (Table 2). In addition, sEV mode size was negatively correlated with hip circumference (Table 2). There was no correlation between sEV size and age (Table 2) or other clinical parameters such as insulin, HOMA, cholesterol levels or blood pressure (not shown).

Interestingly, sEV size expressed as mode or mean was significantly increased in women independently of MetS (Supplemental Fig. 2A, B). However, independently on the gender, sEV size measured as mean decreased with the number of MetS criteria (Supplemental Fig. 2C).

The total number of circulating sEVs was significantly increased in patients with MetS compared to nMetS subjects (Fig. 1G). Interestingly, circulating sEV concentration was positively correlated with weight, waist and hip circumferences, BMI, glycaemia, insulinemia, HOMA, triglyceridemia and LDL cholesterol levels (Fig. 1H–P) but not with age ($r = 0.1053$; $p = 0.3854$). However, sEV concentration was not different between men and women, independently of MetS criteria (Supplemental Fig. 2D).

These results suggest that circulating sEV concentration increases with obesity, insulin resistance and dyslipidemia while size of sEVs decreases with obesity, glycemia and triglyceridemia. Thus, circulating rate and size of sEVs can be correlated with metabolic disorders associated with MetS.

3.4. MetS-sEVs reduce NO release in human endothelial cells and impair endothelium-dependent relaxation of mouse aorta

sEVs were internalized by endothelial cells 4 h after treatment. sEVs from nMetS and MetS patients displayed similar localization around the nucleus of HAoECs after 24 h of treatment (Fig. 2A).

Once internalized, sEVs can affect endothelial function including NO production. MetS-sEVs, in comparison to nMetS-sEVs, caused ~50% reduction of NO production in endothelial cells (Fig. 2B). To explain this decrease, we analyzed by Western blot expression and phosphorylation of enzymes linked to NO pathway. sEVs from both nMetS and MetS patients did not significantly modify the expression of eNOS nor eNOS phosphorylation on its activator site (Ser 1177) in endothelial cells (Fig. 2C) and in mesenteric arteries from sEV-injected mice (Fig. 2F). However, sEVs from MetS, but not from nMetS subjects, increased eNOS phosphorylation at the inhibitor site (Thr 495) in both HAoECs (Fig. 2D) and mesenteric arteries from mice (Fig. 2G) suggesting an inhibitory effect of MetS-sEVs on eNOS activity. In addition, neither nMetS-nor MetS-sEVs significantly modified the insulin-induced AKT phosphorylation in HAoECs (Fig. 2E) indicating that the impairment of NO production is not linked to alterations in the insulin pathway. Finally, intravenous injection of nMetS- and MetS-sEVs in mice did not modify contraction to U46619 of aortas compared to vehicle (data not shown). However, relaxation to acetylcholine was significantly impaired in aortas taken from mice subjected to intravenous injection of MetS-sEVs compared to those from mice injected with either vehicle or nMetS-sEVs ($E_{max} = 53 \pm 3\%$, $65.5 \pm 3\%$, and $67.5 \pm 3\%$, respectively) (Fig. 2H). Otherwise, pD₂ in response to acetylcholine were unchanged between aorta from control mice and mice injected with nMetS-and MetS-sEVs (6.8 ± 0.3 , 6.9 ± 0.4 and 6.6 ± 0.4 , respectively), suggesting that both sEVs subtypes did not modify vascular sensitivity to acetylcholine. In order to determine the functionality of vascular smooth muscle cells (VSMC), we evaluated the endothelial-independent relaxation of aorta to the NO donor, sodium nitroprusside (SNP) that acts directly on VSMC. Relaxation to SNP was not different between the aortas from mice injected with nMetS-, MetS-sEVs or vehicle (Supplemental data, Fig. 3). Altogether these results suggest that sEVs from MetS patients induce endothelial dysfunction related with a decreased NO production in cultured HAoECs and in mouse aorta.

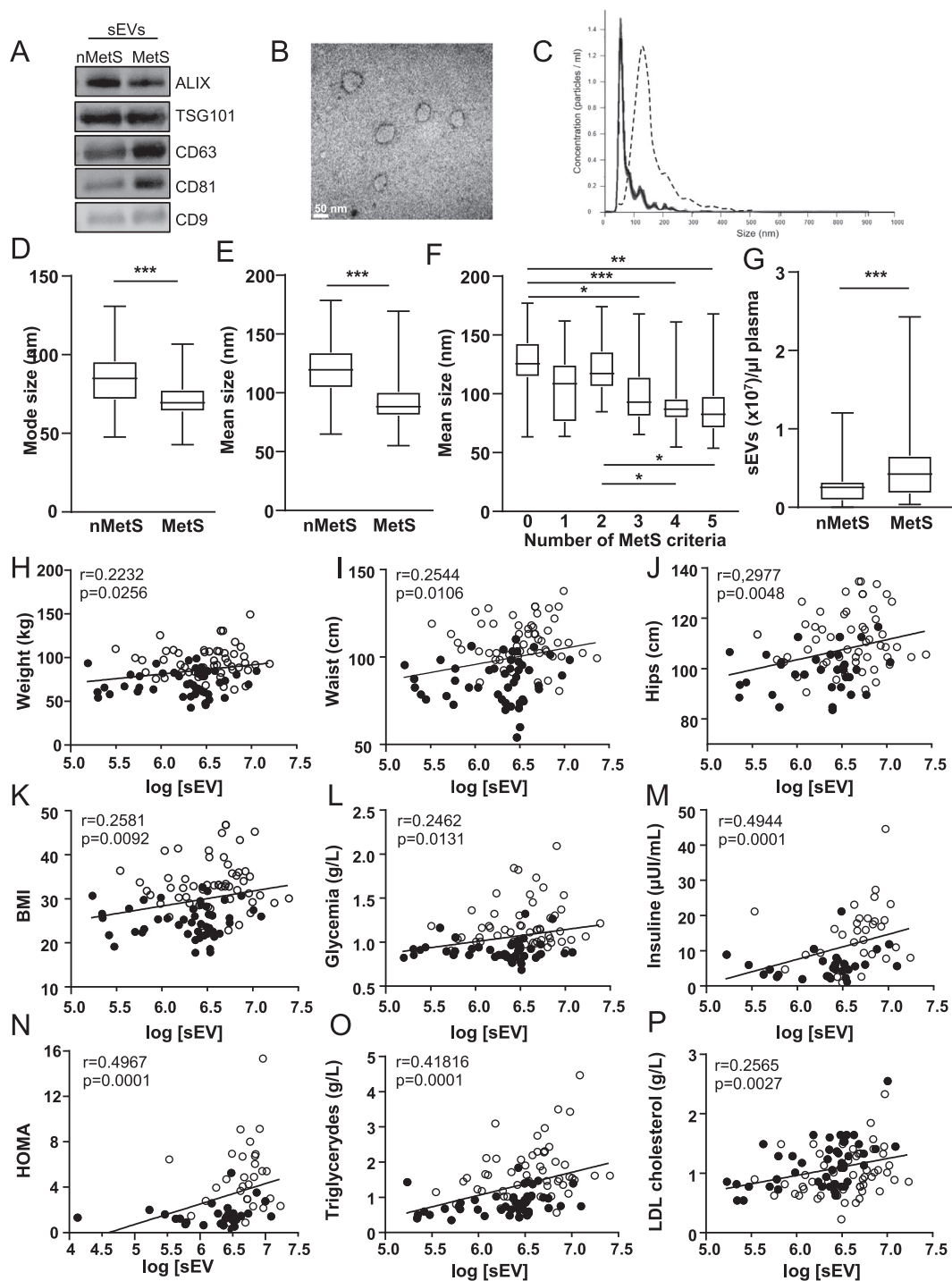


Fig. 1. Characterization of circulating sEVs. (A) Western blotting using antibodies against ALIX, CD63, TSG101, CD81 and CD9 in circulating sEVs both from nMetS and MetS patients. (B) Electron-microscopic observation of isolated sEVs from a MetS patient showing specific round shape and average size of ~60 nm vesicles. (C) Example of curves obtained by NTA, corresponding to sample of a nMetS patient (dotted curve) and a MetS patient (black curve). The graph represents concentration of sEVs (particles/ml) according to the size (nm). (D) sEVs size of nMetS and MetS patients expressed as mode (nm). (E) sEVs size of nMetS and MetS patients expressed as mean (nm). (F) Changes on sEV size expressed as mean (nm) depending on the number of MetS criteria. (G) Circulating concentration of sEVs from nMetS and MetS patients. (H–P) Spearman correlations between circulating sEV concentration (expressed in base 10 logarithm) and weight (H), waist circumference (I), hip circumference (J), BMI (K), glycemia (L), insulinemia (M), HOMA (N), triglycerides (O) and LDL cholesterol levels (P) of patients. MetS patients are illustrated as white circles. * $P < 0.05$; ** $P < 0.01$; *** $P < 0.001$.

3.5. MetS-sEVs increase mitochondrial oxidative stress and decrease NO bioavailability without affecting mitochondrial biogenesis

As illustrated in Fig. 3A and B, EPR analyzes showed that sEVs from MetS patients, but not from nMetS, increased ROS production at 4 h but not at 24 h. Interestingly, incubation with the mitochondrial ROS scavenger mitoTEMPO reduced the early increase of cytosolic ROS

production (Fig. 3C). The participation of mitochondrial ROS in the reduction of NO production by MetS-sEVs on endothelial cells was tested in the presence of mitoTEMPO. Decreased NO release induced by MetS-sEVs was abolished by mitoTEMPO (Fig. 3D). These results suggest that early alteration of mitochondrial function with respect to ROS production participates to decreased NO bioavailability and leads to endothelial dysfunction.

Table 2

Correlations between the sEV size expressed as mode and mean and the anthropometric and biochemical parameters of patients.

	Mode (nm)	Mean (nm)
Age	$r = -0.1298$; $p = 0.189$ (NS)	$r = -0.1100$; $p = 0.2639$ (NS)
Weight	$r = -0.2906$; $p = 0.0031$	$r = -0.3319$; $p = 0.0006$
Waist	$r = -0.3053$; $p = 0.0018$	$r = -0.3853$; $p < 0.0001$
Hip	$r = -0.2195$; $p = 0.0387$	$r = -0.1897$; $p = 0.0733$ (NS)
BMI	$r = -0.3097$; $p = 0.0015$	$r = -0.3774$; $p < 0.0001$
Glycemia	$r = -0.2883$; $p = 0.0031$	$r = -0.3265$; $p = 0.0007$
Triglycerides	$r = -0.3904$; $p < 0.0001$	$r = -0.4495$; $p < 0.0001$

NS = not significant.

In order to explain the increased levels of mitochondrial ROS, we analyzed the effect of sEVs on mitochondrial biogenesis and dynamic in endothelial cells. MetS-sEVs did not modify mitochondrial DNA/total DNA (mtDNA/nDNA) ratio (Supplemental Fig. 4A) nor citrate synthase activity, as an indicator of mitochondrial content (Supplemental Fig. 4B). In addition, MetS-sEVs did not change the expression of PGC1 α (Supplemental Fig. 4C), responsible to the establishment of mitochondrial biogenesis. Also, no significant effects on fusion-associated proteins Mfn1, Mfn2 and OPA1 and fission-associated protein Fis1 were observed (Supplemental Fig. 4D–G). Altogether these data suggest that sEVs from MetS evoke mitochondrial ROS production without affecting mitochondrial biogenesis and dynamic.

3.6. TLR4 activation triggers the increase of oxidative stress induced by sEVs from MetS patients

To determine the intracellular sources of oxidative stress induced by sEVs from MetS patients, endothelial cells were incubated with DHE (targeting cytosolic ROS) or MitoSox (targeting mitochondrial ROS). Whereas nMetS-sEVs did not modify ROS content, MetS-sEVs significantly increased both cytosolic and mitochondrial ROS after 4 h of treatment (Fig. 4A–C). Similar effects were obtained after LPS treatment of HAoECs as positive control (Fig. 4A–C). A link between ROS production and TLR4 activation has been described in MetS [12]. We observed that TLR4 expression in HAoECs was not modified by sEV treatments (Supplemental Fig. 5A). Moreover, neither nMetS- nor MetS-sEVs modified TLR4 expression in mouse mesenteric arteries (Supplemental Fig. 5B). Interestingly, although sEVs did not affect TLR4 expression in HAoECs, TLR4 blockade with TAK-242 prevented the increase in both cytosolic and mitochondrial ROS induced by MetS-sEVs (Fig. 4A–C). In the same way, silencing TLR4 expression by siRNA (Fig. 4D) completely prevented the cytosolic and mitochondrial ROS production induced by both LPS and MetS-sEVs in HAoECs (Fig. 4E–G).

3.7. LPS-enriched MetS-sEVs induce TLR4-dependent ROS production

Among the TLR4 activators, endogenous gut derived-LPS has been proposed to be moderately elevated during metabolic diseases [12]. Thus, we measured the plasma levels of circulating LPS in both MetS and nMetS subjects. MetS patients displayed significantly higher plasma LPS concentration than nMetS subjects (Fig. 5A). Furthermore, we analyzed whether sEVs carry LPS, and we showed that MetS-sEVs were enriched in LPS (Fig. 5B) when compared to those from nMetS subjects. Thereafter, to evaluate the contribution of LPS carried by sEVs on the

production of ROS, we pre-incubated the MetS-sEVs for 1 h with polymyxin B, which blocks the biological effect of LPS, before HAoEC treatment. Under these conditions, neutralization of LPS carried by sEVs prevented the production of both cytosolic and mitochondrial ROS induced by MetS-sEVs (Fig. 5C, D). Finally, we analyzed whether the modification of LPS expression in mesenteric arteries by sEVs injected into mice. As shown in Supplemental Fig. 5C, sEVs from MetS patients, but not those from nMetS subjects, increased LPS expression in mesenteric arteries. Also, under these conditions, MitoSox labelling, but not DHE, was associated with a trend to increase in aorta from mice treated with MetS-sEVs, whereas nMetS-sEVs had no effect on oxidative stress in vessels (Supplemental Fig. 5D).

4. Discussion

Here, we have shown that circulating concentration and size of sEVs were, positively or negatively respectively, correlated with anthropometric and biochemical parameters associated with MetS including visceral obesity, hypertension, insulin resistance and dyslipidemia. Furthermore, sEVs from MetS patients decreased *in vitro* NO production in endothelial cells and impaired *ex vivo* endothelium-dependent relaxation. The decreased NO bioavailability induced by MetS-sEVs was associated with an increase of cytosolic and mitochondrial ROS production without affecting mitochondrial biogenesis and/or dynamic. Interestingly, activation of TLR4 by LPS carried by MetS-sEVs account for the increased oxidative stress evoked by these sEVs. Altogether, these findings suggest that, on the one hand, sEVs can be considered as biological markers of the MetS, and on the other hand, sEVs can be responsible, at least in part, of the low endotoxemia-induced oxidative stress described in MetS patients.

MetS patients used in the present study displayed all the criteria of this syndrome including greater visceral obesity, increased blood pressure and triglyceridemia, and decreased HDL cholesterol. Insulinemia, fasting glycemia, and calculated HOMA were increased arguing for insulin resistance in MetS patients. As shown in Table 1, MetS patients were significantly older than nMetS patients. It is known that the prevalence of MetS increases with age [13,14], however, neither concentration nor size of sEVs were correlated with age, suggesting that ageing does not account for the changes in circulating levels and size of sEVs of MetS patients included in this middle-aged cohort.

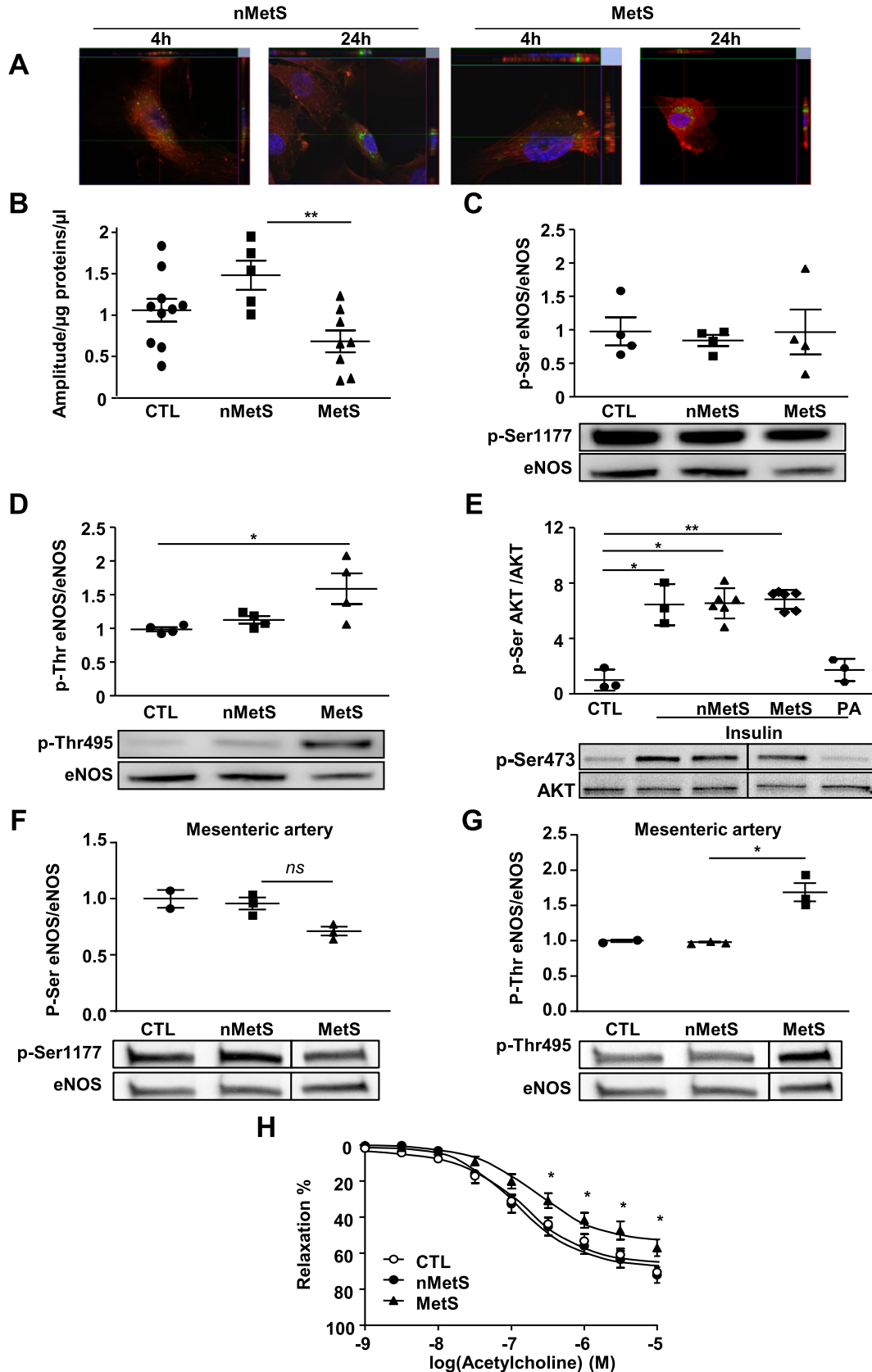
Thereafter, we have shown that circulating concentration of sEVs was increased in MetS patients and positively correlated with factors associated with obesity such as weight, waist and hip circumferences and BMI, with glycemia and insulinemia, and with dyslipidemia. In this respect, it has been reported that levels of fat-derived sEVs were increased with obesity and were principally involved in insulin resistance signaling [15,16]. In agreement with the present data, circulating levels of sEVs were also increased in obese *ob/ob* mice [17], in obese [18] and in diabetic patients [19]. Together, these data suggest that sEVs may be potential biomarkers for the development of obesity-associated metabolic complications such as insulin resistance.

Size of sEVs was negatively correlated with visceral obesity, BMI, glycemia and levels of triglycerides. A recent study demonstrated that plasma sEVs of obese patients are smaller than those from non-obese patients. In addition to BMI, the decrease in sEV size was also negatively correlated with parameters of MetS such as waist circumference, triglyceride levels as well as insulin resistance [20]. However, the

Fig. 2. sEVs from MetS patients decrease *in vitro* NO production in endothelial cells and impair *ex vivo* endothelium-dependent relaxation. (A) Internalization of sEVs from nMetS and MetS patients by endothelial cells. Observation with confocal microscopy of sEVs labeled with PKH67 (green), nucleus with DAPI (blue) and actin with phalloidin (red) was performed at 4 and 24 h. (B) During 24 h, HAoECs were untreated (control) or incubated with nMetS or MetS sEVs (10 μ g/ml) and, then, NO production was measured by electronic paramagnetic resonance. (C–G) Representative immunoblot and quantification of phospho-eNOS Serine 1177 (C), phospho-eNOS Threonine 495 (D) and phospho-Akt Serine 473 (E) induced by nMetS-sEVs or MetS-sEVs in the absence or in the presence of insulin in HAoECs. Palmitic acid (PA) was used as positive control of insulin resistance. (F, G) Representative immunoblot and quantification of phospho-eNOS Serine 1177 (F), phospho-eNOS Threonine 495 (G) induced either by nMetS or MetS-sEVs in mesenteric arteries from female mice. A black line was inserted on the immunoblots when samples were loaded on the same gel, but not side by side. (H) Male mice were injected with vehicle (CTL), nMetS or MetS sEVs (10 μ g/ml) by intravenous injection for 24 h, then aorta ring relaxation was analyzed by myography. Results are expressed as a percentage of relaxation of U46619-induced pre-contraction ($n = 5$ /group). * $P < 0.05$; ** $P < 0.01$. (For interpretation of the references to colour in this figure legend, the reader is referred to the web version of this article.)

mechanisms involved in the differences of sEV size between nMetS and MetS remains to be investigated. In fact, the size of EVs depends not only on the type of membrane phospholipids but also on the presence or

absence of particular membrane proteins [21]. Also, it has been shown that silencing Rab27a, a protein involved in the biogenesis of multivesicular bodies, induced an increase of multivesicular bodies



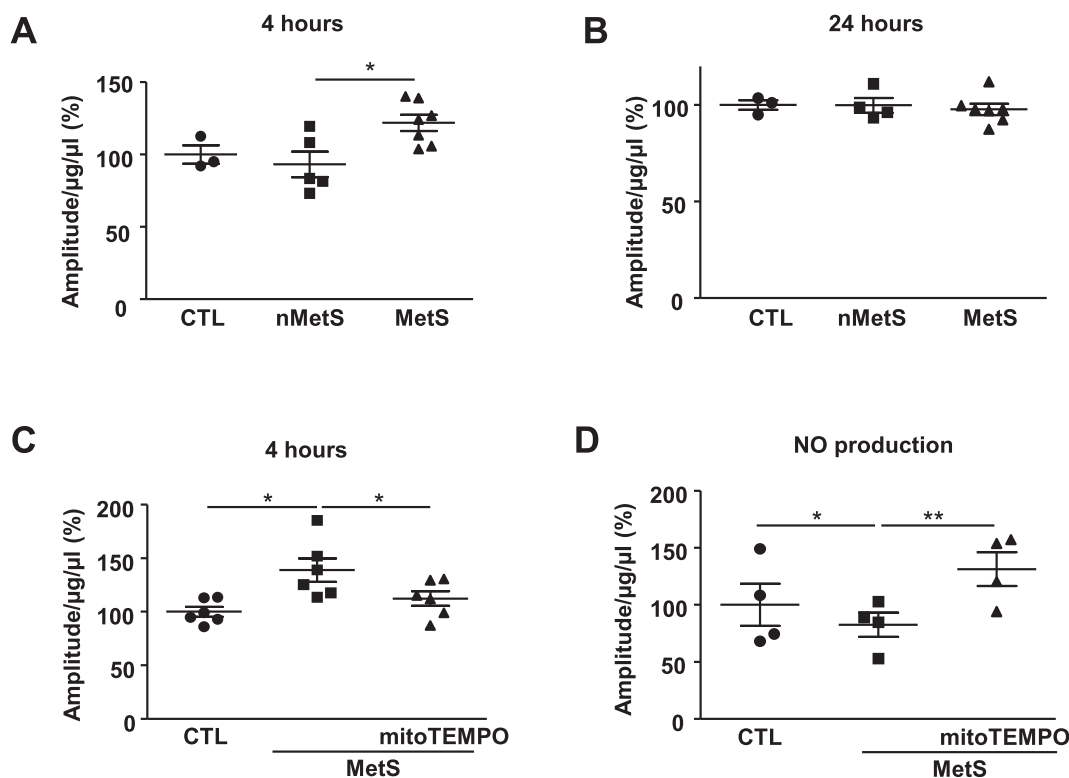


Fig. 3. sEVs from MetS patients increase mitochondrial oxidative stress in endothelial cells. HAoECs were untreated (control) or incubated with 10 $\mu\text{g}/\text{ml}$ of sEVs from nMetS and MetS patients during 4 or 24 h. O_2^- production measured by electronic paramagnetic resonance at 4 h or 24 h (B). (C) O_2^- production measured by electronic paramagnetic resonance in HAoECs incubated for 4 h with MetS-sEVs in absence or presence of mitoTEMPO. (D) NO production measured by electronic paramagnetic resonance in HAoECs incubated with MetS-sEVs in absence or presence of mitoTEMPO. * $P < 0.05$, ** $P < 0.01$.

size [22]. Since the cellular origin of sEVs isolated from plasma can be multiple, it is likely that a common conserved mechanism involved in the sEV biogenesis over different cells producing sEVs is affected in MetS.

Interestingly, sEVs from women were bigger than those from men whereas sEV concentration was independent of gender suggesting the involvement of different mechanisms of sEV biogenesis in men and women. However, since the decrease on size of sEVs was associated with the severity of MetS, that is, the number of MetS criteria, independently of gender, this suggests that MetS is mandatory for the decrease in sEV size.

Endothelial dysfunction is the primary event leading to the impairment of vasodilator, anti-coagulant, and anti-inflammatory effects of healthy endothelium. The most important mechanism for endothelial dysfunction is the decrease in NO availability [23]. Here, we showed that, in HAoECs, MetS-sEVs decreased NO production by increasing phosphorylation on the inhibitor site (Thr 495) of eNOS without affecting AKT pathway activation induced by insulin. Similar results were obtained in mesenteric arteries from female mice injected with sEVs. In addition, MetS-sEVs impaired endothelium-dependent relaxation in aorta of male mice, demonstrating that these vesicles promote endothelial dysfunction independently of the gender of animals receiving sEVs. SNP-induced relaxation was not affected by sEV treatment confirming that the impairment of relaxation induced by acetylcholine was not associated to an alteration of NO sensitivity of the vascular smooth muscle layer. In agreement with these data, we have previously demonstrated that IEVs also induced endothelial dysfunction *in vitro* by decreasing NO production and increasing the inhibitory phosphorylation of eNOS and *in vivo* by decreasing acetylcholine-induced relaxation in mouse aorta [5]. These findings suggest that both types of EVs, IEVs and sEVs, can directly and jointly act on endothelium and, evoke endothelial dysfunction in MetS patients.

The bioavailability of NO depends not only on its generation but also on ROS production. In this respect, MetS-sEV treatment induced an early increase of oxidative stress 4 h after cell treatment by increasing cytosolic and mitochondrial ROS production which further reduced NO availability without any modification of ROS production at 24 h in cells. Also, at 24 h of sEV treatment, cytosolic ROS production was not modified, whereas oxidative stress in mitochondria was associated with a trend to increase *in vivo* in mouse aorta. Unlike MetS-sEVs, endothelial dysfunction induced by MetS-IEVs involved the production of cytosolic ROS at 4 h and mitochondrial ROS at 24 h [6]. These results suggest that sEVs and IEVs affect differentially the spatial and temporal regulation of ROS generation, being mitochondrial ROS induced by sEVs earlier than those by IEVs. It has been reported that, in endothelial cells, the exposition to high glucose altered mitochondrial dynamics which was associated with increased mitochondrial ROS production and a generalized impairment in NO bioavailability [24]. However, the present study shows that the excess of ROS production did not originate from a defect in the mitochondrial biogenesis nor from a modification of the expression of proteins involved in the mitochondrial dynamics. Interestingly, inhibition of mitochondrial ROS production by the mitochondrial ROS scavenger, mitoTEMPO, improved NO bioavailability. These results provide evidence that early mitochondrial ROS production blunted the NO production measured at 24 h. Whether this is due to mitochondrial ROS scavenging effect or their action on NO pathway itself needs further clarification. During endothelial dysfunction, ROS are generated by complexes I and III of the electron transport chain in the mitochondria [25] and by dysregulation of the enzymatic activity of NADPH oxidase [26]. As already described, mitochondrial ROS production can be stimulated by several dangers' signals including activation of membrane TLRs [27] which can also interact with NADPH oxidase and activate ROS generation by those enzymes [28].

Among TLRs, TLR4 is a class of plasma membrane receptors for LPS of Gram-negative bacteria [29]. These receptors have been described as

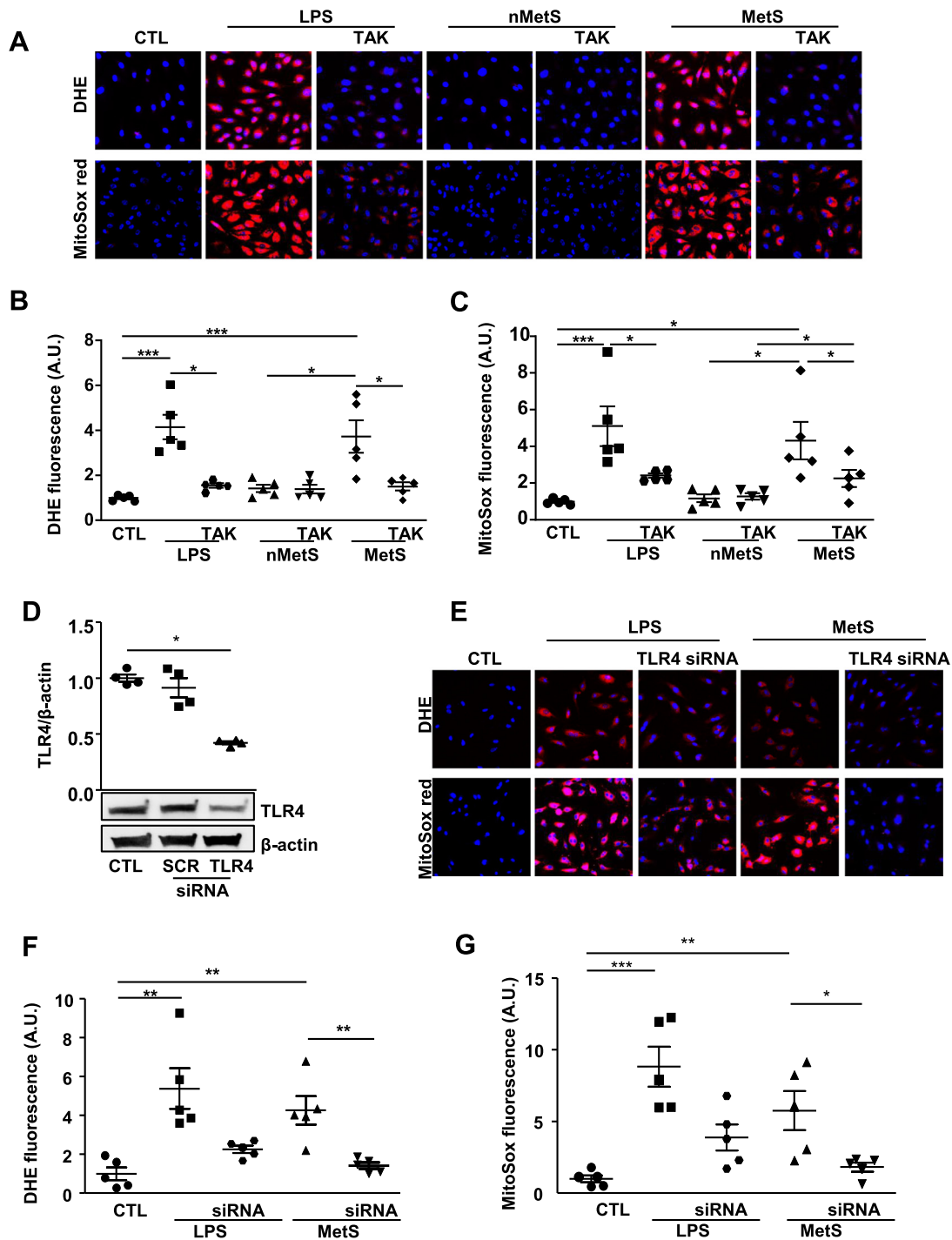


Fig. 4. TLR4 activation triggers the increase of oxidative stress induced by sEVs from MetS patients. Cytosolic ROS production measured by DHE staining (A, B) and mitochondrial ROS production measured by MitoSox labeling (A, C). Cells were incubated with the TLR4 inhibitor TAK-242 during 1 h and then treated with LPS, nMetS-sEVs or MetS-sEVs for 4 h. (D) Expression of TLR4 in cells transfected with siRNA against TLR4 or scrambled siRNA (SCR). (E–G) Cytosolic ROS and mitochondrial ROS productions of cells transfected with TLR4 siRNA, and then treated with LPS or MetS-sEVs for 4 h. * $P < 0.05$; ** $P < 0.01$; *** $P < 0.001$.

playing a major role in the regulation of inflammatory-associated diseases such as atherosclerosis and vascular complications linked to diabetes and obesity [29,30]. In the present study, we show that MetS-sEVs did not modify TLR4 expression in endothelial cells or in mouse arteries. Conversely, blocking TLR4 activity in HAoECs by its inhibitor TAK-242 prevented the cytosolic and mitochondrial ROS production induced by MetS-sEVs. These results suggest that these vesicles did not modulate TLR4 expression but activate TLR4 pathway. Since LPS

is the major activator of TLR4 signaling pathway, and an inducer of mitochondrial ROS production as well as an activator of NADPH oxidase [31], we analyzed endotoxin level in patients' plasma and whether sEVs carry LPS. Indeed, we demonstrated an increase in LPS plasma levels reflecting the presence of endotoxemia in MetS patients. In addition, we observed an enrichment of LPS on sEVs from MetS patients compared to nMetS subjects suggesting that sEVs can account, at least in part, for the endotoxemia described during MetS. Most importantly,

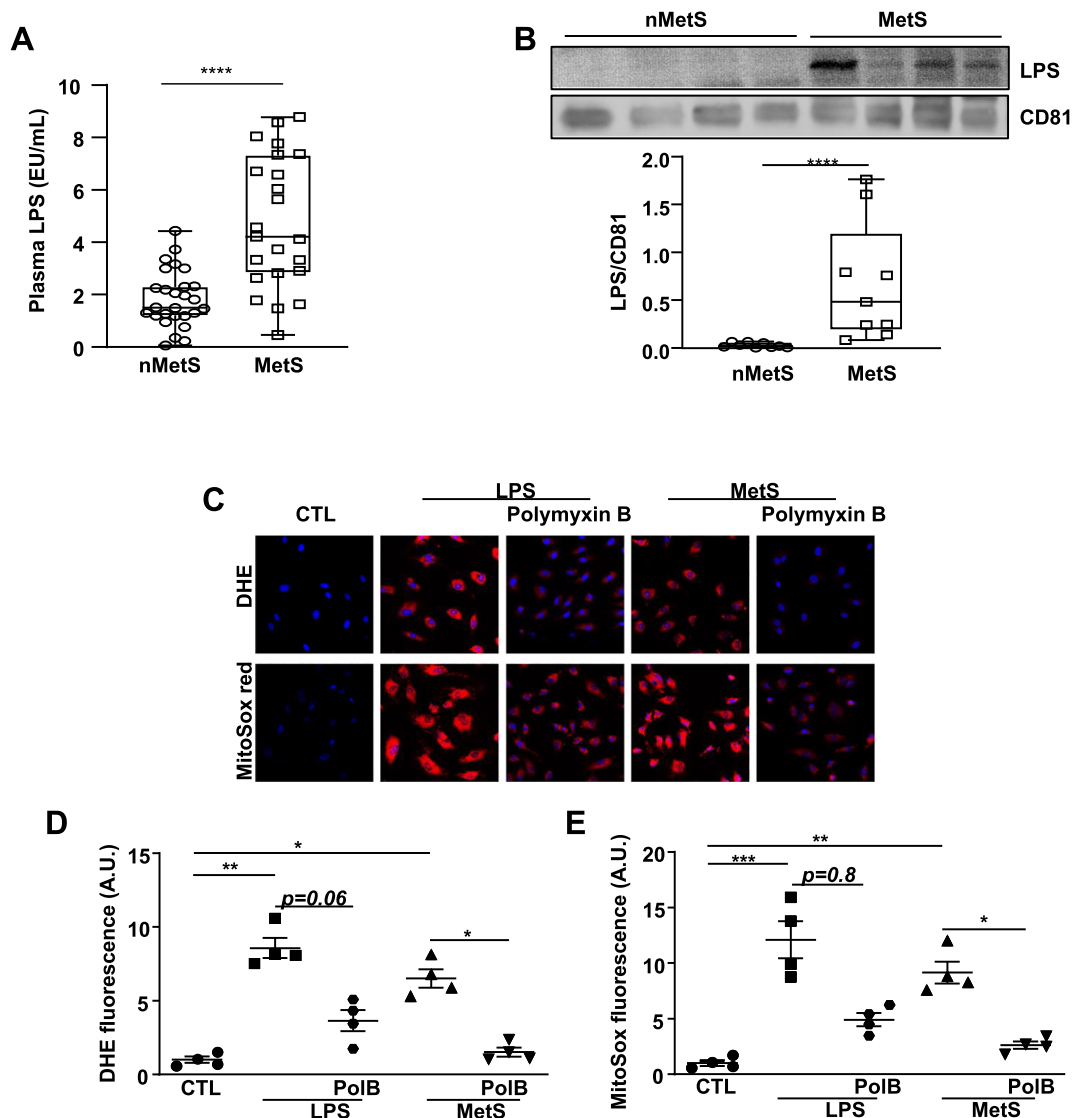


Fig. 5. MetS-sEVs enriched with LPS activate TLR4-induced cytosolic and mitochondrial oxidative stress in endothelial cells. (A) Plasmatic LPS concentration of nMetS or MetS patients. LPS concentration was expressed in endotoxin unit per milliliter (EU/mL). (B) Representative immunoblot and quantification of LPS expression in nMetS-sEVs and MetS-sEVs. CD81 was used as control of loaded proteins. (C–E) Cytosolic and mitochondrial ROS productions of human endothelial cells incubated or not with polymyxin B (PoIB) during 1 h, and then, treated with LPS or MetS-sEVs for 4 h. * $P < 0.05$; ** $P < 0.01$; *** $P < 0.001$.

the direct inhibition of LPS carried by sEVs by its inhibitor polymyxin B prevented both cytosolic and mitochondrial ROS production in endothelial cells.

In line with these findings, mice fed with high-fat diet displayed an increase of low-grade elevation in plasma LPS, which was associated with changes in gut microbiota and permeability, being responsible for the onset of metabolic diseases including increased oxidative stress [32–34]. Furthermore, endotoxemia has been proposed to be associated with the development of cardiovascular diseases such as atherosclerosis [35–37]. Similar findings have been reported providing evidence that the LPS-TLR4 axis is responsible of metabolic disturbances in obese and diabetic patients [38] in association with an elevation in circulating endotoxin [39] and gut microbiota alterations [40]. Here, we showed for the first time that sEVs from MetS carry LPS and activate TLR4 pathway to induce endothelial dysfunction. It has been reported that LPS can be pelleted during ultracentrifugation [41,42] using higher speed and duration than those used in the present work (150,000g, 4.5 h, 150,000g for 1 h, versus 100,000g, 70 min). Although we cannot exclude that LPS might be precipitated during the isolation of EVs, this amount of pelleted LPS would be very low because of the experimental protocol

used. On the other hand, LPS released from gut bacteria might adhere into surfaces of circulating sEVs. Finally, it is also plausible that we detect LPS associated to outer membrane vesicles (OMVs) released by Gram-negative bacteria [43], since OMVs from gut bacteria can cross the epithelial barrier as a consequence of altered intestinal barrier integrity and induce inflammation or metabolic disorders to the host, such as insulin resistance [44,45]. In line with our data, a very recent study clearly demonstrates increased levels of systemic LPS-positive EVs in patients with intestinal barrier dysfunction. Indeed, LPS-positive EVs are present in plasma, are able to induce immune activation and correlate with impaired barrier integrity in patients diagnosed with intestinal bowel disease [46]. Nevertheless, we showed that circulating sEVs from MetS patients carry LPS and may contribute to metabolic endotoxemia leading to endothelial dysfunction in these patients.

4.1. Limitations

Although the number of animals used in the present study is low, suggesting low power analysis, the described effects are statistically significant. In addition, in order to follow the international convention

regarding the reduction of the number of animals used, we stopped experiments when significant differences were reached. Also, we found differences in the age of nMetS and MetS patients. Although age was not correlated with sEV concentration or size, it should be noted that age has a significant impact on endothelial function and sEVs from old individuals may affect the observed effects. Even MetS is being diagnosed in more and more young population, the incidence of MetS increases with age.

5. Conclusions

In summary, the present data reveal that LPS-enriched sEVs, probably from gut microbiota, can be involved in the development of endothelial dysfunction in MetS through the activation of TLR4 and the generation of both mitochondrial and cytosolic ROS leading to decreased NO availability, promoting vascular damage and cardiovascular diseases in these patients. These results and those previously obtained with IEVs from MetS patients showing that MetS-IEVs induced endothelial dysfunction through the activation of the Fas/Fas ligand pathway and endoplasmic reticulum stress associated with an increase of oxidative stress [6], reinforce the notion that both types of circulating EVs from MetS patients are the link between the endothelial dysfunction and metabolic disturbances in MetS.

Supplementary data to this article can be found online at <https://doi.org/10.1016/j.metabol.2021.154727>.

CRedit authorship contribution statement

Sakina Ali: Investigation, Formal analysis, Writing – original draft, Writing – review & editing, Visualization. **Marine Mallocci:** Investigation, Formal analysis, Writing – original draft. **Zainab Safiedeen:** Investigation, Formal analysis. **Raffaella Soletti:** Investigation, Formal analysis. **Luisa Vergori:** Investigation, Formal analysis. **Xavier Vidal-Gómez:** Investigation, Formal analysis, Funding acquisition. **Charlène Besnard:** Investigation, Formal analysis. **Séverine Dubois:** Resources. **Soazig Le Lay:** Investigation. **Jérôme Boursier:** Resources. **Arnaud Chevrollier:** Investigation. **Frédéric Gagnadoux:** Resources. **Gilles Simard:** Resources. **Ramaroson Andriantsitohaina:** Conceptualization, Resources, Writing – review & editing, Funding acquisition. **M. Carmen Martinez:** Conceptualization, Validation, Resources, Supervision, Writing – review & editing, Visualization, Funding acquisition.

Acknowledgments

We thank SCAHU staff (Université d'Angers) for taking care of animals, and SCIAM staff (Université d'Angers) for electronic microscopy observation and the staff of Centre Hospitalo-Universitaire d'Angers who compose the METABOL Group for analysis of clinical data of NUMEVOX cohort. This work was supported by Institut National de la Santé et de la Recherche Médicale, Université d'Angers, Centre Hospitalo-Universitaire d'Angers. SA and MM were recipients of a doctoral fellowship from Conseil Départemental de Mayotte and INSERM-Pays de La Loire, respectively. XVG was supported by Fondation pour la Recherche Médicale (SPF201809006985).

Metabol study group composition

CLINICS (Centre Hospitalo-Universitaire d'Angers (CHU), Angers, France).

- Hepatology: Jérôme Boursier, Paul Calès, Frédéric Oberti, Isabelle Fouchard-Hubert, Adrien Lannes
- Diabetology: Séverine Dubois, Ingrid Allix, Pierre-Henri Ducluzeau
- Pneumology: Frédéric Gagnadoux, Wojciech Trzepizur, Nicole Muesli, Pascaline Priou
- Functional Vascular Explorations: Samir Henni, Georges Leftheriotis,

- Pierre Abraham
- Radiology: Christophe Aubé

BASIC SCIENCE (INSERM U1063, SOPAM, Angers University, France).
Ramaroson Andriantsitohaina, M Carmen Martinez, Soazig Le Lay, Raffaella Soletti, Luisa Vergori.
STATISTICS: Gilles Hunault.
BIOLOGICAL RESSOURCE CENTER: Odile Blanchet, Belaid Sekour.
COORDINATION: Jean-Marie Chrétien, Sandra Girre.

Author contributions

SA, MM, ZS, RS, LV, XVG, CB, conducted experiments, acquired data, analyzed data; SD, JB, FG, GS provided human samples; SLL, AC, discussed the study; GS, RA, MCM conceived and supervised the study; SA, MCM designed the experiments; SA, MM, MCM wrote the manuscript.

References

- [1] Tziomalos K, Athyros VG, Karagiannis A, Mikhailidis DP. Endothelial dysfunction in metabolic syndrome: prevalence, pathogenesis and management. *Nutr Metab Cardiovasc Dis.* 2010;20:140–6.
- [2] Chistiakov DA, Orekhov AN, Bobryshev YV. Extracellular vesicles and atherosclerotic disease. *Cell Mol Life Sci.* 2015;72:2697–708.
- [3] Martínez MC, Andriantsitohaina R. Extracellular vesicles in metabolic syndrome. *Circ Res.* 2017;120:1674–86.
- [4] Mallocci M, Perdomo L, Veerasamy M, Andriantsitohaina R, Simard G, Martínez MC. Extracellular vesicles: mechanisms in human health and disease. *Antioxid Redox Signal.* 2019;30:813–56.
- [5] Agouni A, Lagrue-Lak-Hal AH, Ducluzeau PH, Mostefai HA, Draunet-Busson C, Leftheriotis G, et al. Endothelial dysfunction caused by circulating microparticles from patients with metabolic syndrome. *Am J Pathol.* 2008;173:1210–9.
- [6] Safiedeen Z, Rodríguez-Gómez I, Vergori L, Soletti R, Vaithilingam D, Douma I, et al. Temporal cross talk between endoplasmic reticulum and mitochondria regulates oxidative stress and mediates microparticle-induced endothelial dysfunction. *Antioxid Redox Signal.* 2017;26:15–27.
- [7] Lee MJ, Park DH, Kang JH. Exosomes as the source of biomarkers of metabolic diseases. *Ann Pediatr Endocrinol Metab.* 2016;21:119–25.
- [8] Kranendonk ME, de Kleijn DP, Kalkhoven E, Kanhai DA, Uiterwaal CS, van der Graaf Y, et al. Extracellular vesicle markers in relation to obesity and metabolic complications in patients with manifest cardiovascular disease. *Cardiovasc Diabetol.* 2014;13:37.
- [9] Karolina DS, Tavintharan S, Armugam A, Sepramaniam S, Pek SL, Wong MT, et al. Circulating miRNA profiles in patients with metabolic syndrome. *J Clin Endocrinol Metab.* 2012;97:E2271–6.
- [10] Huber HJ, Holvoet P. Exosomes: emerging roles in communication between blood cells and vascular tissues during atherosclerosis. *Curr Opin Lipidol.* 2015;26:412–9.
- [11] Alberti KGM, Eckel RH, Grundy SM, Zimmet PZ, Cleeman JI, Donato KA, et al. Harmonizing the metabolic syndrome: a joint interim statement of the international diabetes federation task force on epidemiology and prevention; National Heart, Lung, and Blood Institute; American Heart Association; world heart federation; international atherosclerosis society; and International Association for the Study of obesity. *Circulation.* 2009;120:1640–5.
- [12] Boutagy NE, McMillan RP, Frisard MI, Hulver MW. Metabolic endotoxemia with obesity: is it real and is it relevant? *Biochimie.* 2016;124:11–20.
- [13] Hildrum B, Mykletun A, Hole T, Midthjell K, Dahl AA. Age-specific prevalence of the metabolic syndrome defined by the international diabetes federation and the National Cholesterol Education Program: the Norwegian HUNT 2 study. *BMC Public Health.* 2007;7:220.
- [14] Park E, Kim J. Gender- and age-specific prevalence of metabolic syndrome among Korean adults: analysis of the fifth Korean National Health and nutrition examination survey. *J Cardiovasc Nurs.* 2015;30:256–66.
- [15] Deng Z, Poliakov A, Hardy RW, Clements R, Liu C, Liu Y, et al. Adipose tissue exosome-like vesicles mediate activation of macrophage-induced insulin resistance. *Diabetes.* 2009;58:2498–505.
- [16] Hubal MJ, Nadler EP, Ferrante SC, Barberio MD, Suh JH, Wang J, et al. Circulating adipocyte-derived exosomal MicroRNAs associated with decreased insulin resistance after gastric bypass. *Obesity.* 2017;25:102–10.
- [17] Phoonsawat W, Aoki-Yoshida A, Tsuruta T, Sonoyama K. Adiponectin is partially associated with exosomes in mouse serum. *Biochem Biophys Res Commun.* 2014;448:261–6.
- [18] Amosse J, Durcin M, Mallocci M, Vergori L, Fleury A, Gagnadoux F, et al. Phenotyping of circulating extracellular vesicles (EVs) in obesity identifies large EVs as functional conveyors of macrophage migration inhibitory factor. *Mol Metab.* 2018;18:134–42.
- [19] Freeman DW, Noren Hooten N, Eitan E, Green J, Mode NA, Bodogai M, et al. Altered extracellular vesicle concentration, cargo, and function in diabetes. *Diabetes.* 2018;67:2377–88.

- [20] Santamaria-Martos F, Benitez ID, Latorre J, Lluch I, Moreno-Navarrete JM, Sabater M, et al. Comparative and functional analysis of plasma membrane-derived extracellular vesicles from obese vs. nonobese women. *Clin Nutr.* 2019;29:1067–76.
- [21] Margolis L, Sadovsky Y. The biology of extracellular vesicles: the known unknowns. *PLoS Biol.* 2019;17:7.
- [22] Ostrowski M, Carmo NB, Krumeich S, Fanget I, Raposo G, Savina A, et al. Rab27a and Rab27b control different steps of the exosome secretion pathway. *Nat Cell Biol.* 2010;12:19–30.
- [23] Favero G, Paganelli C, Buffoli B, Rodella LF, Rezzani R. Endothelium and its alterations in cardiovascular diseases: life style intervention. *Biomed Res Int.* 2014;2014:801896.
- [24] Shenouda SM, Widlansky ME, Chen K, Xu G, Holbrook M, Tabit CE, et al. Altered mitochondrial dynamics contributes to endothelial dysfunction in diabetes mellitus. *Circulation.* 2011;124:444–53.
- [25] Snezhkina AV, Kudryavtseva AV, Kardymon OL, Savvateeva MV, Melnikova NV, Krasnov GS, et al. ROS generation and antioxidant defense systems in normal and malignant cells. *Oxid Med Cell Longev.* 2019;6175804.
- [26] Montezano AC, Touyz RM. Reactive oxygen species and endothelial function – role of nitric oxide synthase uncoupling and Nox family nicotinamide adenine dinucleotide phosphate oxidases. *Basic Clin Pharmacol Toxicol.* 2012;110:87–94.
- [27] West AP, Brodsky IE, Rahner C, Woo DK, Erdjument-Bromage H, Tempst P, et al. TLR signalling augments macrophage bactericidal activity through mitochondrial ROS. *Nature.* 2011;472:476–80.
- [28] Park HS, Jung HY, Park Y, Kim J, Lee WJ, Bae YS. Cutting edge: direct interaction of TLR4 with NAD(P)H oxidase 4 isozyme is essential for lipopolysaccharide-induced production of reactive oxygen species and activation of NF- κ B. *J Immunol.* 2004;173:3589–93.
- [29] Shi H, Kokoeva MV, Inouye K, Tzameli I, Yin H, Flier JS. TLR4 links innate immunity and fatty acid-induced insulin resistance. *J Clin Invest.* 2006;116:3015–25.
- [30] Lu Z, Li Y, Jin J, Zhang X, Lopes-Virella MF, Huang Y. Toll-like receptor 4 activation in microvascular endothelial cells triggers a robust inflammatory response and cross talk with mononuclear cells via interleukin-6. *Arterioscler Thromb Vasc Biol.* 2012;32:1696–706.
- [31] Simon F, Fernández R. Early lipopolysaccharide-induced reactive oxygen species production evokes necrotic cell death in human umbilical vein endothelial cells. *J Hypertens.* 2009;27:1202–16.
- [32] Cani PD, Amar J, Iglesias MA, Poggi M, Knauf C, Bastelica D, et al. Metabolic endotoxemia initiates obesity and insulin resistance. *Diabetes.* 2007;56:1761–72.
- [33] Cani PD, Bibiloni R, Knauf C, Waget A, Neyrinck AM, Delzenne NM, et al. Changes in gut microbiota control metabolic endotoxemia-induced inflammation in high-fat diet-induced obesity and diabetes in mice. *Diabetes.* 2008;57:1470–81.
- [34] Cani PD, Possemiers S, Van de Wiele T, Guiot Y, Everard A, Rottier O, et al. Changes in gut microbiota control inflammation in obese mice through a mechanism involving GLP-2-driven improvement of gut permeability. *Gut.* 2009;58:1091–103.
- [35] Awoyemi A, Trøseid M, Arnesen H, Solheim S, Seljeflot I. Markers of metabolic endotoxemia as related to metabolic syndrome in an elderly male population at high cardiovascular risk: a cross-sectional study. *Diabetol Metab Syndr.* 2018;10:59.
- [36] Loffredo L, Ivanov V, Ciobanu N, Deseatinicova E, Gutu E, Mudrea L, et al. Is there an association between atherosclerotic burden, oxidative stress, and gut-derived lipopolysaccharides? *Antioxid Redox Signal.* 2020;33:761–6.
- [37] Yang G, Wei J, Liu P, Zhang Q, Tian Y, Hou G, et al. Role of the gut microbiota in type 2 diabetes and related diseases. *Metabolism.* 2021. <https://doi.org/10.1016/j.metabol.2021.154712> (in press).
- [38] Reyna SM, Ghosh S, Tantiwong P, Meka CS, Eagan P, Jenkinson CP, et al. Elevated toll-like receptor 4 expression and signaling in muscle from insulin-resistant subjects. *Diabetes.* 2008;57:2595–602.
- [39] Kallio KA, Hätönen KA, Lehto M, Salomaa V, Männistö S, Pussinen PJ. Endotoxemia, nutrition, and cardiometabolic disorders. *Acta Diabetol.* 2015;52:395–404.
- [40] Ley RE, Turnbaugh PJ, Klein S, Gordon JL. Human gut microbes associated with obesity. *Nature.* 2006;444:1022–3.
- [41] Vesly CJ, Kitchens RL, Wolfbauer G, Albers JJ, Munford RS. Lipopolysaccharide-binding protein and phospholipid transfer protein release lipopolysaccharides from gram-negative bacterial membranes. *Infect Immun.* 2000;68:2410–7.
- [42] Ingalls RR, Lien E, Golenbock DT. Membrane-associated proteins of a lipopolysaccharide-deficient mutant of *Neisseria meningitidis* activate the inflammatory response through toll-like receptor 2. *Infect Immun.* 2001;69:2230–6.
- [43] Macia L, Nanan R, Hosseini-Beheshti E, Grau GE. Host- and microbiota-derived extracellular vesicles, immune function, and disease development. *Int J Mol Sci.* 2019;21:107.
- [44] Ellis TN, Kuehn MJ. Virulence and immunomodulatory roles of bacterial outer membrane vesicles. *Microbiol Mol Biol Rev.* 2010;74:81–94.
- [45] Choi Y, Kwon Y, Kim D, Jeon J, Jang S, Wang T, et al. Gut microbe-derived extracellular vesicles induce insulin resistance, thereby impairing glucose metabolism in skeletal muscle. *Sci Rep.* 2015;5:15878.
- [46] Tulkens J, Vergauwen G, Van Deun J, Geeurickx E, Dhondt B, Lippens L, et al. Increased levels of systemic LPS-positive bacterial extracellular vesicles in patients with intestinal barrier dysfunction. *Gut.* 2020;69:191–3.